Leukocyte Protease Binding to Nucleic Acids Promotes Nuclear Localization and Cleavage of Nucleic Acid Binding Proteins

Marshall P. Thomas, Jennifer Whangbo, Geoffrey McCrossan, Aaron J. Deutsch, Kimberly Martinod, Michael Walch and Judy Lieberman

J Immunol 2014; 192:5390-5397; Prepublished online 25 April 2014;
doi: 10.4049/jimmunol.1303296
http://www.jimmunol.org/content/192/11/5390

The Journal of Immunology is published twice each month by
The American Association of Immunologists, Inc.,
9650 Rockville Pike, Bethesda, MD 20814-3994.

Print ISSN: 0022-1767 Online ISSN: 1550-6606.

Leukocyte Protease Binding to Nucleic Acids Promotes Nuclear Localization and Cleavage of Nucleic Acid Binding Proteins

Marshall P. Thomas,[1] Jennifer Whangbo,[1] Geoffrey McCrossan, Aaron J. Deutsch, Kimberly Martinod, Michael Walch,[2] and Judy Lieberman

Killer lymphocyte granzyme (Gzm) serine proteases induce apoptosis of pathogen-infected cells and tumor cells. Many known Gzm substrates are nucleic acid binding proteins, and the Gzms accumulate in the target cell nucleus by an unknown mechanism. In this study, we show that human Gzms bind to DNA and RNA with nanomolar affinity. Gzms cleave their substrates most efficiently when both are bound to nucleic acids. RNase treatment of cell lysates reduces Gzm cleavage of RNA binding protein targets, whereas adding RNA to recombinant RNA binding protein substrates increases in vitro cleavage. Binding to nucleic acids also influences Gzm trafficking within target cells. Preincubation with competitor DNA and DNase treatment both reduce Gzm nuclear localization. The Gzms are closely related to neutrophil proteases, including neutrophil elastase (NE) and cathepsin G. During neutrophil activation, NE translocates to the nucleus to initiate DNA extrusion into neutrophil extracellular traps, which bind NE and cathepsin G. These myeloid cell proteases, but not digestive serine proteases, also bind DNA strongly and localize to nuclei and neutrophil extracellular traps in a DNA-dependent manner. Thus, high-affinity nucleic acid binding is a conserved and functionally important property specific to leukocyte serine proteases. Furthermore, nucleic acid binding provides an elegant and simple mechanism to confer specificity of these proteases for cleavage of nucleic acid binding protein substrates that play essential roles in cellular gene expression and cell proliferation. ***The Journal of Immunology*****, 2014, 192: 5390–5397.**

Cytotoxic T lymphocytes and NK cells eliminate virus-infected cells and tumor cells by releasing the granzyme (Gzm) serine proteases and perforin from cytotoxic granules into the immunologic synapse formed with the cell destined for elimination (1). GzmA and GzmB, the most abundant and best-studied Gzms, are delivered to the target cell cytosol by perforin, rapidly concentrate in the target cell nucleus by an unknown mechanism, and induce independent programs of cell death (2, 3). To orchestrate cell death in diverse types of target cells, the Gzms cleave multiple substrates, likely numbering in the hundreds, within the cytosol, nucleus, and mitochondria (1, 4). DNA and RNA binding proteins are highly represented in the set of Gzm substrates. All but 1 of the 17 substrates of GzmA that have been carefully validated bind to DNA, RNA, or chromatin (1, 4). A recent proteomics study that profiled GzmA substrates in isolated nuclei identified 44 candidate substrates, of which 33 were RNA binding proteins (RBPs), including 12 heterogeneous nuclear ribonucleoproteins (hnRNP) (4). The remaining 11 candidate substrates were mostly DNA-binding proteins. In some cases, the nucleic acid appears to play an important role in the Gzm–target interaction. GzmA cleavage of histone H1 (H1) and binding to poly [ADP-ribose] polymerase 1 depends on the presence of DNA (5, 6). All five of the human Gzms cleave hnRNP K in an RNA-dependent manner (7). Gzm cleavage of viral and host nucleic acid binding proteins also plays an important role in controlling viral infection (8, 9). Thus many of the substrates of GzmA and GzmB are nucleic acid binding proteins that are physiologically important for cytotoxicity or the control of viral infections.

Although serine proteases have a high degree of sequence similarity, the Gzms are most closely related to a group of myeloid cell granule proteases involved in microbial defense. These immune proteases include the neutrophil proteases neutrophil elastase (NE) and cathepsin G (CATG) (10). When neutrophils are activated, they can ensnare and kill microbes in neutrophil extracellular traps (NETs), which are formed by nuclear DNA in a unique, non-apoptotic cell death mechanism called NETosis (11). NE participates in NETosis by translocating to the neutrophil nucleus, where it cleaves histones (12). Histone cleavage promotes chromatin decondensation, which precipitates the extrusion of nuclear DNA through the cell membrane. The extruded DNA is coated with histones, antimicrobial peptides, NE, and CATG (13).

The aim of this study was to explore further the role of nucleic acids in mediating Gzm–substrate interactions and trafficking. We

Program in Cellular and Molecular Medicine, Boston Children's Hospital, Boston, MA 02115; Division of Hematology-Oncology, Boston Children's Hospital, Boston, MA 02215; and Department of Pediatrics, Harvard Medical School, Boston, MA 02115

[1]M.P.T. and J.W. contributed equally to this work.

[2]Current address: Department of Medicine, Anatomy Unit, University of Fribourg, Fribourg, Switzerland.

Received for publication December 9, 2013. Accepted for publication March 24, 2014.

This work was supported by a National Science Foundation graduate research fellowship (to M.P.T.), National Institutes of Health K08 Grant HL094460 (to J.W.), a Boston Children's Hospital Career Development Fellowship (to J.W.), and National Institutes of Health Grant AI45587 (to J.L.).

Address correspondence and reprint requests to Dr. Judy Lieberman or Dr. Jennifer Whangbo, Harvard Medical School, WAB 255, 200 Longwood Avenue, Boston, MA 02115 (J.L.) or Boston Children's Hospital/Dana-Farber Cancer Institute, 450 Brookline Avenue, Boston, MA 02215 (J.W.). E-mail addresses: judy.lieberman@childrens.harvard.edu (J.L.) or jennifer.whangbo@childrens.harvard.edu (J.W.)

The online version of this article contains supplemental material.

Abbreviations used in this article: AF488, Alexa Fluor 488; CATG, cathepsin G; CI, confidence interval; FP, fluorescence polarization; GO, gene ontology; Gzm, granzyme; H1, histone H1; hnRNP, heterogeneous nuclear ribonucleoprotein; NE, neutrophil elastase; NET, neutrophil extracellular trap; pI, isoelectric point; RBP, RNA binding protein; RT, room temperature.

www.jimmunol.org/cgi/doi/10.4049/jimmunol.1303296

find that RNA enhances in vitro cleavage of RBP substrates, but not non-RBP substrates. We show that Gzms directly bind RNA and DNA with nanomolar affinity. NE and CATG also bind nucleic acids with high affinity, whereas digestive serine proteases do not. In the presence of competitor DNA, the leukocyte serine proteases do not localize to nuclei and NETs. Together, our findings indicate that nucleic acid binding is a conserved and functionally important property of leukocyte serine proteases that directs them to and enhances their cleavage of nucleic acid binding protein targets.

Materials and Methods

Abs

The following Abs were used at the indicated final concentration or dilution: mouse mAbs to hnRNP U (3G6; Santa Cruz Biotechnology; 0.2 μg/ml), hnRNP A1 (4B10; Sigma-Aldrich; 2 μg/ml), lamin B1 (101-B7; Calbiochem; 1/1,000), α-tubulin (B-5-1-2; Sigma-Aldrich; 1/1000), G3BP1 (23/G3BP; BD Biosciences; 0.25 μg/ml), hnRNP C1/C2 (4F4; Sigma-Aldrich; 0.4 μg/ml), β-actin (Developmental Studies Hybridoma Bank; 1/1000), HuR (3A2; Santa Cruz Biotechnology; 0.2 μg/ml); rabbit antisera to HMGB2 (Abcam; 1/1000), ICAD (Abcam; 0.5 μg/ml), and NE (Abcam; 1 μg/ml); and DDX5 (Abcam; 0.5 μg/ml). Secondary Abs were sheep anti-mouse HRP (GE Healthcare; 1/2500), donkey anti-rabbit HRP (GE; 1/2500), donkey anti-goat HRP (GE Healthcare; 1/2500), goat anti-rabbit Alexa Fluor 488 (AF488; Invitrogen; 1/200), and donkey anti-mouse Cy3 (715-165-150; Jackson ImmunoResearch Laboratories; 1:200). Normal rabbit IgG (2729; Cell Signaling Technology; 1 μg/ml) was used as an isotype control for immunofluorescence.

Proteins

Human GzmA and GzmB expression plasmids (4) were transfected into HEK 293T cells by calcium phosphate precipitation. The transfected cells were grown in serum-free ExCell 293 medium (Sigma-Aldrich) for 4 d. Recombinant Gzms were purified from the culture supernatants by immobilized metal affinity chromatography using Nickel-NTA (Qiagen) following the manufacturer's instructions. Eluted Gzms were treated with enterokinase (0.05 IU/ml supernatant; Sigma-Aldrich) for 16 h at room temperature (RT). Active Gzms were finally purified on an S column, concentrated, and quality tested as previously described (14). GST-tagged HuR, hnRNPC1, and LMNB1 were expressed and purified as described (4). H1 (M2501S; New England Biolabs) and caspase-3 (ALX-201-059-U025; Enzo Life Sciences) were purchased. Other serine proteases were NE (16-14-051200; Athens Research and Technology, Athens, GA), pancreatic elastase (324682; Millipore), CATG (16-14-030107; Athens Research and Technology), and trypsinogen (T1143; Sigma-Aldrich). Proteins were fluorescently labeled with AF488 according to the manufacturer's instructions (A30006; Invitrogen).

In vitro cleavage in cell lysates

Whole-cell lysates were made from 10^6 HeLa cells suspended in 1 ml lysis buffer (50 mM Tris-HCl [pH 8] and 100 mM NaCl) by alternating freezing in an ethanol/dry ice bath and thawing at 37°C three times. Cell debris was pelleted by centrifugation (16,000 × *g* for 10 min at 4°C). The supernatant was divided, and half was treated with RNase A/T1 (Thermo Scientific) at a concentration of 325 U/ml for 30 min at 37°C. RNaseOUT (Invitrogen) was added at a concentration of 1000 U/ml to the remaining half. The lysates were then treated with the indicated amounts of Gzms in a volume of 60 μl for 15 min at 37°C. In some cases, GzmB was incubated with varying amounts of salmon sperm DNA on ice for 30 min before addition to lysates. The cleavage reaction was stopped by adding 5× SDS loading buffer and boiling at 95°C for 5 min. For caspase-3 experiments, lysates were incubated with or without 1 U recombinant capsase-3 for 1 h before stopping the reaction. Samples were analyzed by SDS-PAGE and immunoblot.

In vitro cleavage of recombinant proteins

In vitro cleavage was performed in 100 mM NaCl and 50 mM Tris-HCl (pH 7.5). Each protein was first incubated in the indicated concentration of HeLa cell total RNA or salmon sperm DNA for 20 min and then incubated with 50 nM GzmB for 15 min (hnRNP C), 50 nM GzmB for 30 min (LMNB1), 200 nM GzmA for 20 min (H1), or 5 nM NE for 10 min (H1). Total HeLa cell RNA was purified with TRIzol (Invitrogen) according to the manufacturer's instructions. The final concentrations of hnRNP C, LMNB1, and H1 were 333, 1, and 400 nM, respectively. For HuR cleavage, RNA oligonucleotides were diluted to 10 μM, heated at 70°C for 10 min, and cooled on ice. A total of 400 nM recombinant GST-tagged HuR was incubated with or without 200 nM recombinant GzmB. The cleavage reactions were performed in the presence of 3 ng/μl total HeLa RNA, AU RNA, or BB94 RNA at the indicated molar ratios and incubated in a total volume of 40 μl at 37°C for 30 min. Cleavage reactions were stopped by adding 5× SDS loading buffer and boiling for 5 min. Cleavage was assayed by immunoblot or silver staining (Invitrogen SilverQuest kit; Invitrogen).

Protease localization in permeabilized HeLa cells

HeLa cells were obtained from American Type Culture Collection and maintained in DMEM supplemented with 10% heat-inactivated FBS, 100 U/ml penicillin G, 100 μg/ml streptomycin sulfate, 6 mM HEPES, 1.6 mM L-glutamine, and 50 μM 2-ME. HeLa cells were grown overnight on 12-mm coverslips, then fixed for 10 min at RT in 2% formaldehyde, and permeabilized for 10 min in methanol on dry ice. In some experiments, the cells were treated with DNase I (New England Biolabs) or RNase A/T1 (Thermo Scientific) at a 1:50 dilution for 4 h at RT before blocking. The cells were blocked with 1% BSA in PBS for 1 h at RT, and coverslips were incubated with blocking buffer containing salmon sperm DNA or no DNA for 30 min on ice and then incubated at RT for 1 h with 100 nM AF488-labeled serine proteases. The coverslips were then washed and stained with 4 μg/ml DAPI in PBS and mounted on slides (48311-703; VWR International) using polyvinyl alcohol (P-8136; Sigma-Aldrich) aqueous mounting medium. Cells were imaged using an Axiovert 200M microscope (Pan Apochromat, 1.4 numerical aperture; Carl Zeiss). Images were analyzed with SlideBook 4.2 (Intelligent Imaging Innovations).

Neutrophil isolation and activation

Human studies were reviewed and approved by the Harvard Committee on the Use of Human Subjects (IRB-P00005698). Neutrophils were isolated from the blood of deidentified healthy donors by density-gradient centrifugation as described (15). The neutrophil layer was washed with HBSS and resuspended at 10^6 cells/ml in RPMI 1640. Neutrophils (2.5×10^5) were incubated at 37°C for 15 min on 12-mm coverslips in 24-well flat-bottom cell-culture plates and then treated in 500 μl RPMI 1640 for 3 h with 100 nM PMA (P1585; Sigma-Aldrich). In some experiments, 100 nM AF488-labeled protease and/or salmon sperm DNA (D7656; Sigma-Aldrich) was added just prior to adding PMA. Treated cells were fixed in PBS containing 4% formaldehyde. For immunofluorescence staining of endogenous NE, the fixed cells were incubated with primary Ab or rabbit antiserum control for 1 h at RT, washed three times in PBS, and then incubated in secondary Ab (AF488-labeled goat anti-rabbit IgG) for 1 h at RT. The cells were washed, stained with DAPI, and mounted as above.

Gene ontology and phylogenetic analysis of serine proteases

We analyzed the candidate targets of human GzmA (16) and GzmB (17) identified by proteomics using the FuncAssociate tool (18) on default settings. Top gene ontology (GO) terms were ranked by the sum of the $-\log_{10}(p)$ values for enrichment of targets of each enzyme. All human proteins having the GO term "serine-type peptidase activity" (GO:0008236) were identified with AmiGO (19). Of these proteins, the manually annotated and reviewed Swiss-Prot sequences were downloaded using the UniProt retrieve tool (20). The sequences were trimmed to focus on their protease domains and exclude spurious alignment of other protein domains in multidomain proteins. The ClustalW2 (21) multiple sequence alignment and phylogeny tools were used with default parameters to construct a phylogenetic tree. Phylogeny was visualized with the EvolView Web tool (22).

Fluorescence polarization oligonucleotides

The following FAM-labeled oligonucleotides were used for fluorescence polarization (FP) (all from Integrated DNA Technologies): BB94 DNA, 5′-TCTGTGAGTTGAACGCACACATCACAAAGGAG-FAM-3′; $dA_{(30)}$, 5′-AAAAAAAAAAAAAAAAAAAAAAAAAAAAAA-FAM-3′; $dC_{(30)}$, 5′-CCCCCCCCCCCCCCCCCCCCCCCCCCCCCC-FAM-3′; $dT_{(30)}$, 5′-TTTTTTTTTTTTTTTTTTTTTTTTTTTTTT-FAM-3′; $rU_{(30)}$, 5′-UUUUUUUUUUUUUUUUUUUUUUUUUUUUUU-FAM-3′; BB94 RNA, 5′-UCUGUGAGUUGAACGCACACAUCACAAAGGA-FAM-3′; and AU RNA, 5′-CCCAAGCUUAUUUAUUUAUUUAUUGCAGGUC-FAM-3′.

FP assays

FAM-labeled oligonucleotides were used at 10 nM, and binding reactions were performed in a total volume of 20 μl. Proteins and oligonucleotides were diluted in 10 mM Tris-HCl (pH 7.5), 100 mM NaCl, and 2.5 mM $MgCl_2$. For RNA oligonucleotides, RNAseOUT was added to a final concentration of 1 U/μl. Diluted RNA oligonucleotides were heated to 70°C for 10 min prior to use. In the salt concentration assay, protein concentration was fixed (100 nM), and either NaCl or KCl was added to the

assay buffer at the indicated final concentrations. Samples were equilibrated in 384-well black polystyrene assay plates (3575; Corning) for 20 min at RT, and polarization was determined using a Synergy 2 Microplate Reader and Gen5 Data Analysis Software (BioTek).

FP data analysis

The apparent equilibrium K_d was determined from fitting the data to a sigmoidal dose-response function using JMP Pro 10 (JMP Statistical Discovery Software from SAS Institute). The apparent K_d was determined for each protein–nucleic acid interaction using the equation f = c + {[*d* − c]/[1 + 10^ (−a[$\log_{10}$([P] − b)])]}, where f is the fraction bound or the polarization value, [P] is the protein concentration, b is the equilibrium K_d, a is the Hill coefficient, d is the maximum polarization, and c is the minimum polarization (23). Each experiment was performed at least in duplicate. The average and SE of the polarization value for each protein concentration was calculated from at least 10 independent samples.

Oligo(dT) pulldown

A total of 120 μl Oligo(dT)$_{25}$ Dynabeads (61002; Invitrogen) and 10 μl Protein G Dynabeads (10004D; Invitrogen) was washed three times in 50 mM Tris-HCl (pH 7.5) and 100 nM NaCl. The beads were blocked for 30 min at RT in the same buffer containing 0.5% BSA (A9647; Sigma-Aldrich). Following blocking, half of the Oligo(dT)$_{25}$ Dynabeads were treated at RT for 30 min with 25 U Benzonase Nuclease (E1014; Sigma-Aldrich), and the other half was left untreated. After this incubation, the beads were incubated with 120 μl protein (final concentration 1 μM) in blocking buffer for 30 min at RT. The beads were washed three times, and protein was eluted by boiling samples for 3 min in 30 μl SDS loading buffer. Samples were electrophoresed through a 12% polyacrylamide denaturing gel and visualized by Coomassie staining.

Results

Predicted targets of GzmA and GzmB are enriched for nucleic acid binding proteins

Because the Gzms concentrate in the nucleus of target cells, we hypothesized that proteins that function in the nucleus might be overrepresented among Gzm substrates. Two proteomics studies identified candidate GzmA and GzmB substrates without bias by analyzing Gzm-incubated cell lysates for novel cleavage products

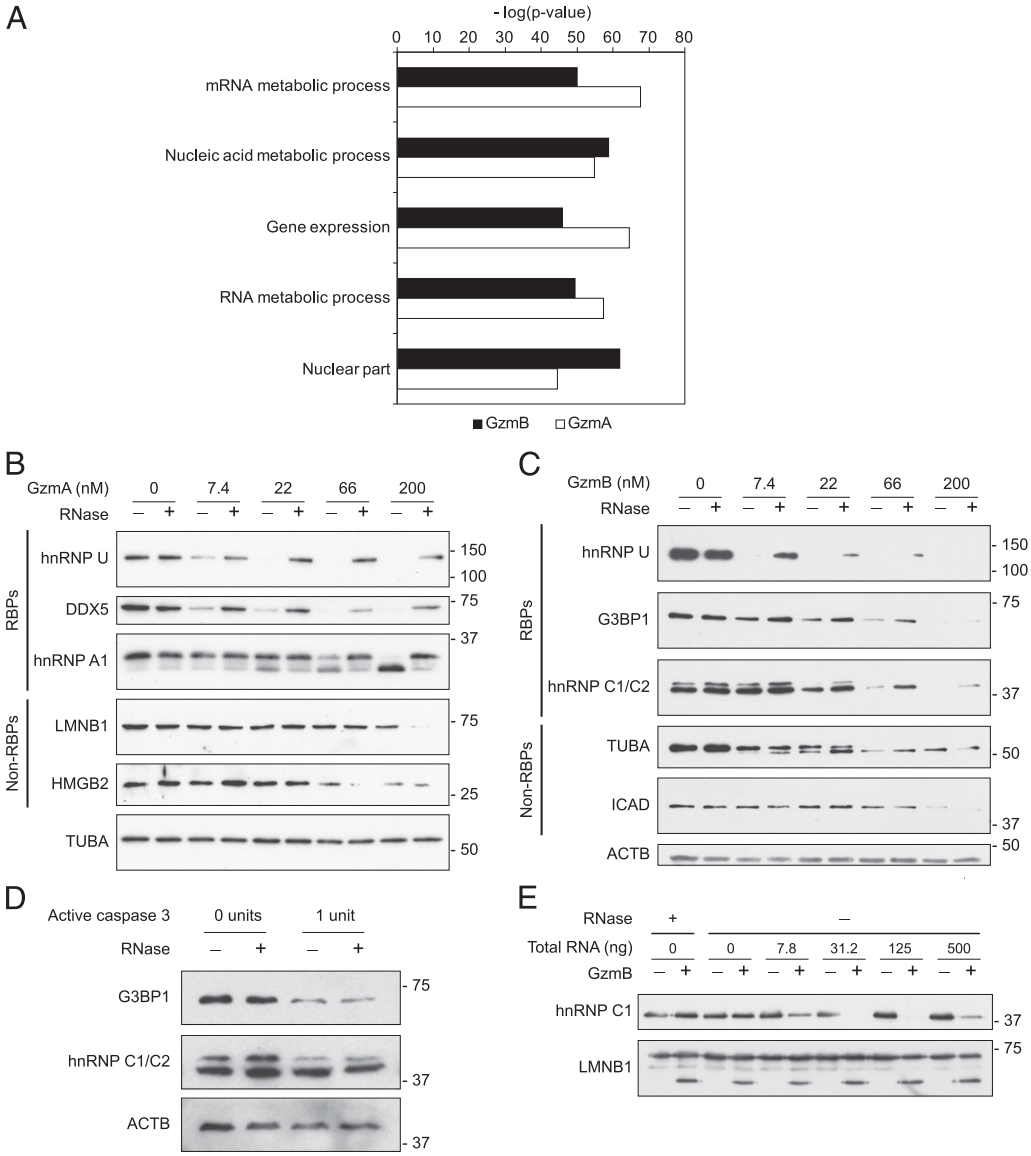

FIGURE 1. RBP target cleavage by Gzms is enhanced by RNA. (**A**) GO analysis of GzmA and GzmB targets. Nucleic acid binding proteins are highly enriched. (**B**–**E**) Cell lysates or recombinant proteins were incubated with RNase or the indicated concentration of total RNA followed by incubation with Gzms or caspase 3. The reactions were analyzed by immunoblot. RNase treatment of HeLa cell lysates reduced cleavage by GzmA (B) and GzmB (C) of RBP targets, but not non-RBP targets. Results in (B) and (C) are representative of at least three independent experiments. (D) RNase treatment of HeLa cell lysates did not affect cleavage of RBP targets by active caspase-3. (E) GzmB cleavage of recombinant hnRNP C1, but not recombinant LMNB1, was enhanced by exogenous total RNA. Results in (D) and (E) are representative of two independent experiments.

(16, 17). We analyzed these target lists using the FuncAssociate GO tool (18) for overrepresented GO terms in both GzmA and GzmB datasets (Fig. 1A, Supplemental Table I). Proteins with nucleic acid–related GO terms were the most highly enriched categories, when analyzed for each Gzm individually or together. The top seven GO terms for both Gzms (mRNA metabolic process, nucleic acid metabolic process, gene expression, RNA metabolic process, nuclear part, nucleotide metabolic process, and RNA binding) were highly significantly overrepresented (p values of $\sim 10^{-50}$ for each Gzm). This analysis suggested that Gzms might have a special preference for nucleic acid binding, especially RBP, substrates.

RNA promotes GzmA and GzmB cleavage of RNA-binding proteins

We first asked whether RNA enhances Gzm RBP cleavage by comparing Gzm cleavage of RBPs in whole-cell lysates depleted of RNA. HeLa cell lysates were pretreated or not with a mixture of RNase A and T1 before a 15-min incubation with varying concentrations of recombinant human GzmA or GzmB. The samples were then immunoblotted for known GzmA and GzmB targets. All three GzmA RBP targets analyzed (hnRNP U, DDX5, and hnRNP A1) were cleaved less efficiently in RNase-treated samples (Fig. 1B). Similarly, cleavage of RBP targets of GzmB (hnRNP U, G3BP1, and hnRNP C1/C2) was reduced by removing RNA (Fig. 1C). In contrast, non-RBP targets (LMNB1, HMGB2, TUBA, and ICAD) were cleaved equally or more efficiently in RNase-treated lysates, suggesting that Gzm target preference is altered to favor non-RBPs in the absence of RNA. This effect is not universal to cytotoxic proteases, as RNase treatment did not affect caspase-3 cleavage of hnRNP C1/C2 and G3BP1 RBP substrates (Fig. 1D). We next tested whether adding HeLa cell RNA would alter in vitro GzmB cleavage of recombinant hnRNP C1 and LNMB1. The RBP hnRNP C1 was more efficiently cleaved in the presence of added RNA, whereas cleavage of the non-RBP LMNB1 was unaffected (Fig. 1E). These results indicate that RNA enhances Gzm cleavage of RBP targets. Of note, although the highest concentration of RNA still enhanced cleavage, GzmB cleavage of hnRNP C1 was more efficient when less RNA was added.

The Gzms bind to RNA with nanomolar affinity

Because RNA enhanced Gzm activity against RBPs, we hypothesized that the Gzms might bind to RNA to direct them to RBP targets. We tested RNA binding by FP, a technique widely used to measure protein–nucleic acid interactions (24), using a 3′ FAM-labeled oligouridylate homopolymer (rU_{30}). As a positive control, we measured RNA binding of human Ag R (HuR), a GzmB substrate that binds to AU-rich RNA sequences (25). GzmA, GzmB, and HuR all bound to rU_{30} with high affinity, whereas the negative control protein BSA did not bind (Fig. 2A). The apparent equilibrium K_d of all three purified proteins with the rU_{30} oligonucleotide determined by FP was in the nanomolar range (Table I).

GzmB cleavage of HuR is enhanced by HuR binding to RNA

Because HuR preferentially binds AU-rich sequences, we used its specificity to assess the effect of substrate binding to RNA on GzmB cleavage. We compared GzmB cleavage of HuR in the presence of an AU-rich target sequence (AU RNA) (26) that both HuR and GzmB bind with similar affinity (Fig. 2B, Table I) and in the presence of a control sequence (BB94) that binds well only to GzmB (Fig. 2C, Table I). Formation of the cleavage product was enhanced by AU RNA, but only minimally increased by BB94 RNA (Fig. 2D). These results suggest that RBP targets are optimally cleaved by Gzms when both the target and Gzm interact with RNA.

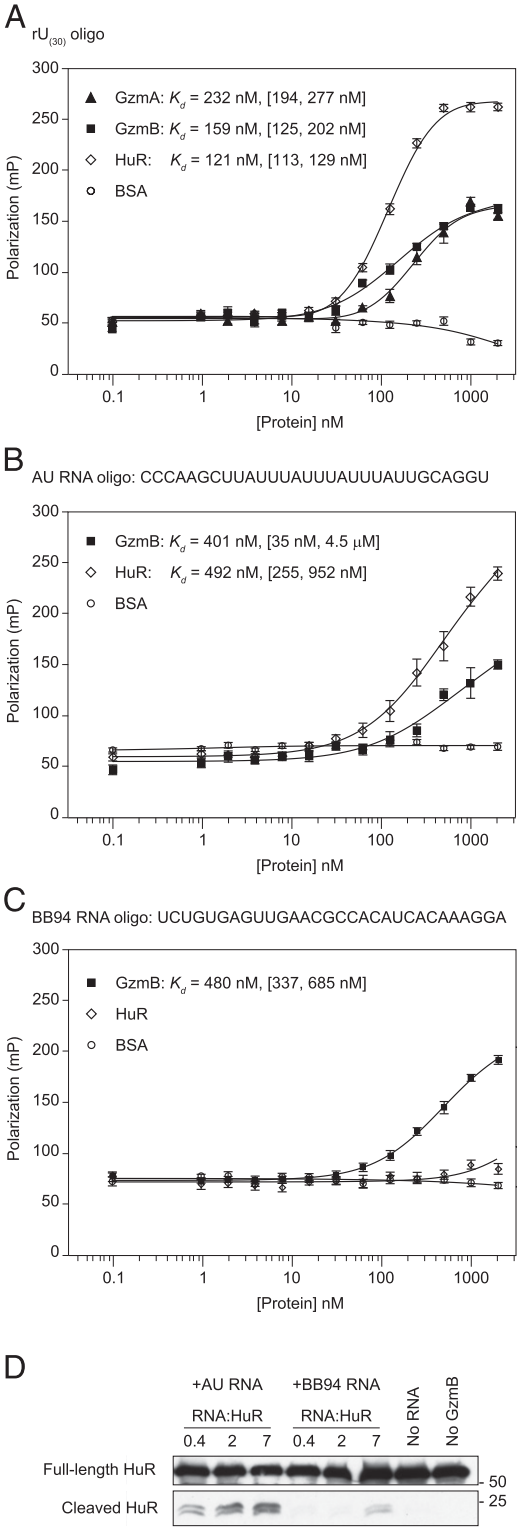

FIGURE 2. Gzms directly bind RNA. FP assays with purified Gzms and RNA. (**A**) GzmA and GzmB bound to a FAM-labeled 30-nt RNA [$rU_{(30)}$]. (**B**) GzmB and HuR bind a 30-nt RNA containing an AU-rich sequence (AU RNA). (**C**) GzmB, but not HuR, binds a length-matched control RNA (BB94 RNA). The mean polarization values ± SEM are plotted, and the apparent K_d with 95% CI in brackets is shown. Results are representative of at least three independent experiments. (**D**) GzmB cleaves HuR, an RBP target, most efficiently when it is bound to RNA. GST-tagged HuR protein was incubated with indicated molar ratios of AU RNA or BB94 RNA, and GzmB was then added for 30 min. HuR cleavage was detected by immunoblot probed for GST.

Table I. Protein–nucleic acid interactions measured by FP in this study

Oligonucleotide	Protein	K_d (nM)
$rU_{(30)}$	GzmA	232 (194–277)
	GzmB	159 (125–202)
	HuR	121 (113–129)
AU RNA	GzmA	401 (35 nM–4.5 μM)
	GzmB	651 (157 nM–2.7 μM)
	NE	602 (304 nM–1.2 μM)
	CATG	165 (139–197)
	HuR	492 (255–952)
BB94 ssRNA	GzmA	1.6 μM (188 nM–15.2 μM)
	GzmB	480 (337–685)
	HuR	4.8 μM (16 nM–1465.9 μM)
BB94 ssDNA	GzmA	122 (95–158)
	GzmB	35 (31–40)
	NE	272 (219–339)
	CATG	22 (17–29)
	H1	10 (8–12)
BB94 dsDNA	GzmA	120 (106–136)
	GzmB	161 (112–231)
	NE	607 (516–712)
	CATG	35 (24–52)
	H1	9 (7–13)
$dC_{(30)}$	GzmA	91 (65–127)
	GzmB	175 (140–219)
$dT_{(30)}$	GzmA	48 (42–55)
	GzmB	45 (26–78)

The apparent K_d with 95% CI in parentheses is given for each binding interaction.

Gzms bind DNA with nanomolar affinity

Because the Gzms bind to RNA and cleave many DNA binding proteins, we asked whether they could also bind DNA. We used FP to measure the binding of GzmA and GzmB to an ssDNA oligonucleotide of the same sequence as BB94 RNA (Fig. 3A). Both GzmA and GzmB bound ssDNA with nanomolar K_d (Table I). GzmB {K_d 35 nM [95% confidence interval (CI) 31–40]} bound ssDNA almost as strongly as H1 (K_d 10 nM [95% CI 8–12]), similar to reported values (27). GzmA binding was somewhat weaker (K_d 122 nM [95% CI 95–158]). Both Gzms also bound to a dsDNA oligonucleotide containing the same BB94 sequence with nanomolar affinities (Fig. 3B). To determine if Gzm binding might have a sequence preference, we performed FP assays with ssDNA homopolymers (dA_{30}, dT_{30}, and dC_{30}). Oligo(dG) was not tested because it tends to form higher order structures and aggregate. Both Gzms bound $dT_{30} > dC_{30}$ with nanomolar affinity, but only weakly bound to dA_{30} (Fig. 3C, 3D). This suggests that the Gzms bind preferentially to pyrimidines. These assays were performed in buffer containing 100 mM NaCl. Because many protein–DNA complexes are sensitive to salt concentration, we performed FP assays over a range of NaCl and KCl concentrations, while holding the GzmB and nucleic acid concentration constant. Although binding decreased at higher salt concentrations, binding of GzmB to DNA and RNA remained strong at physiological concentrations (150 mM NaCl or KCl) (Supplemental Fig. 1).

Myeloid granule serine proteases bind nucleic acids

Next we asked whether nucleic acid binding is a general property of serine proteases or limited to a subset. To visualize the evolutionary relationships between the Gzms and other serine proteases, we performed a phylogenetic analysis of all annotated human serine proteases. The Gzms form a monophyletic group with other leukocyte serine proteases (Fig. 4A). This group includes five neutrophil proteases (NE, CATG, NSP4, PRTN3, and AZU1) (28) and the mast cell protease CMA1. The Gzms are more distantly related to digestive enzymes, such as pancreatic elastase and trypsin. We

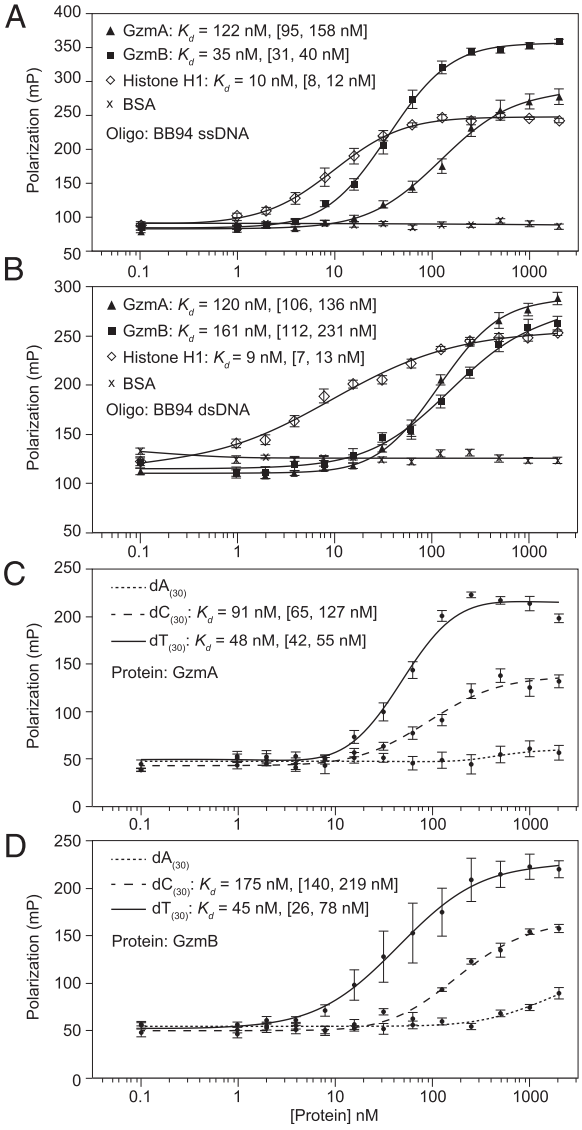

FIGURE 3. GzmA and GzmB bind DNA with nanomolar affinity. The binding of a FAM-labeled ssDNA (**A**) or dsDNA (**B**) oligonucleotide (BB94) to GzmA, GzmB, H1, and BSA was measured by FP. To determine whether binding was sequence dependent, interactions of GzmA (**C**) and GzmB (**D**) with 3′ FAM-labeled homo-oligomers [$dA_{(30)}$, $dC_{(30)}$, and $dT_{(30)}$] were measured by FP. Both Gzms bound pyrimidine tracts [$dT_{(30)}$ and $dC_{(30)}$] more strongly than the purine tract $dA_{(30)}$. The mean polarization values ± SEM are plotted, and the apparent K_d with 95% CI in brackets is shown. Results are representative of at least three independent experiments.

used FP to assess the affinity of native human CATG and NE, porcine pancreatic elastase, and bovine trypsinogen (the proenzyme of trypsin) for RNA, ssDNA, and dsDNA (Fig. 4B). Both neutrophil proteases bound these nucleic acids with nanomolar affinity like the Gzms, but neither digestive protease bound. This agrees with an earlier study showing that NE binds to DNA (29). To validate DNA binding with an independent assay, we used oligo(dT)-conjugated beads to pull down the Gzms, neutrophil proteases, and pancreatic elastase (Fig. 4C). Consistent with the FP results, the leukocyte proteases (GzmA, GzmB, NE, and CATG), but not the digestive protease, bound to oligo(dT) beads. Binding was specific to DNA because it was decreased by pretreating the beads with DNase. The proteases also did not bind to protein G–conjugated beads. We hypothesized that DNA binding

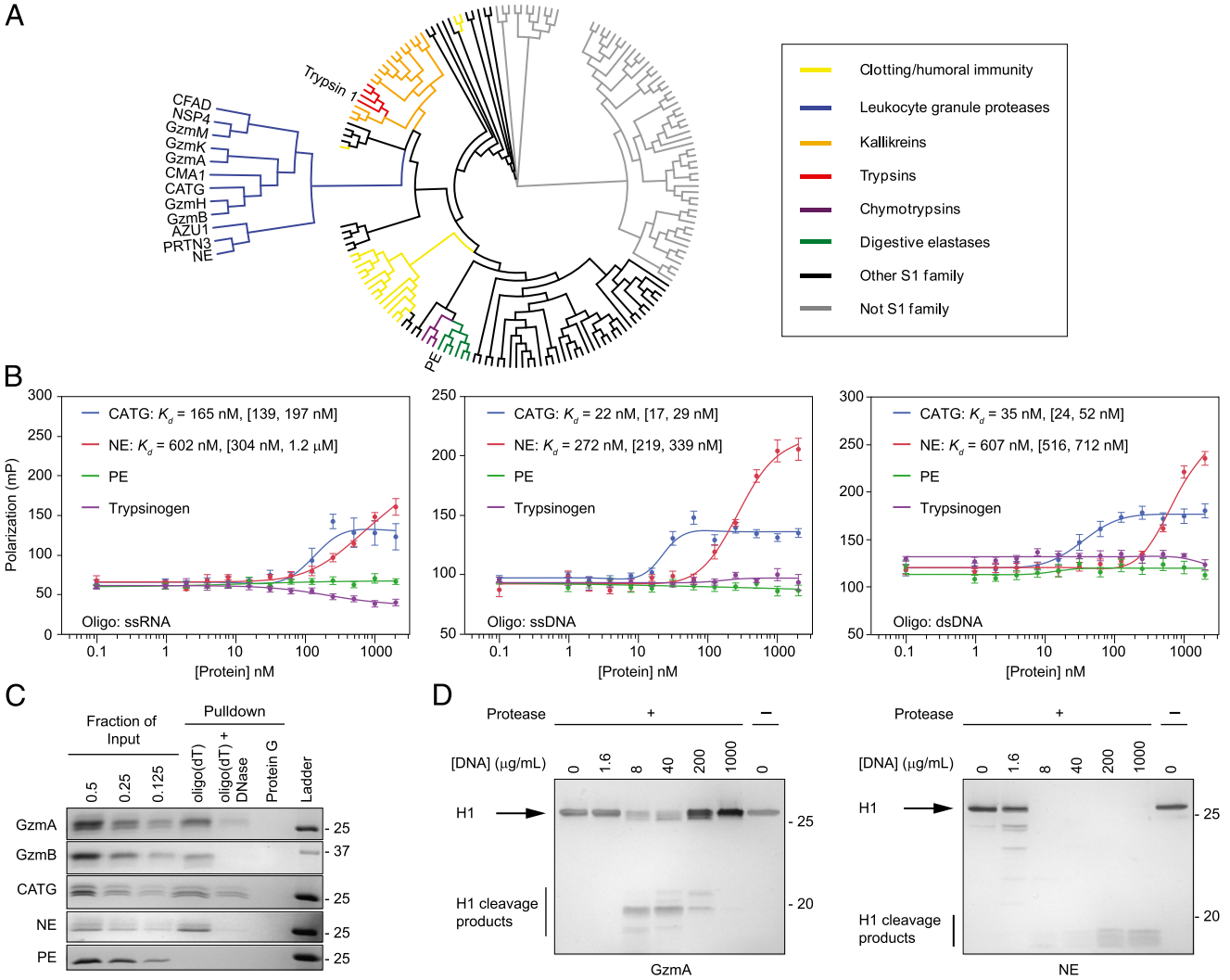

FIGURE 4. Leukocyte serine proteases bind to RNA and DNA with nanomolar affinity. (**A**) Phylogenetic analysis of all human serine proteases shows that leukocyte serine proteases form a monophyletic group. (**B**) Interactions of two neutrophil serine proteases (NE and CATG) and digestive serine proteases (trypsinogen and pancreatic elastase [PE]) with RNA, ssDNA, and dsDNA were measured by FP. NE and CATG bound with nanomolar affinity, but the digestive proteases did not. The mean polarization values ± SEM and the apparent K_d with 95% CI in brackets are shown. (**C**) Direct binding of GzmA, GzmB, NE, CATG, and PE to ssDNA was assessed by affinity pulldown with oligo(dT)$_{25}$-conjugated beads. The leukocyte proteases bound, but the digestive enzyme did not. Binding was reduced by DNase treatment. None of the proteases bound to protein G beads. (**D**) Purified H1 was not cleaved in the absence of added DNA. Cleavage of H1 by GzmA and NE was assessed in the presence of increasing amounts of salmon sperm DNA. Addition of small amounts of DNA enhanced cleavage by both GzmA and NE. At higher concentrations, DNA inhibited GzmA cleavage. Results are representative of at least three independent experiments.

would enhance leukocyte protease cleavage of DNA binding protein substrates, as shown above for RNA and previously shown for GzmA cleavage of H1 (5). We treated purified H1, a target of both GzmA and NE with each protease in the presence of increasing concentrations of salmon sperm DNA. H1 cleavage by NE was greatly increased by adding even a small amount of DNA (Fig. 4D). H1 cleavage by GzmA was first promoted, then inhibited, by increasing amounts of salmon sperm DNA. Inhibition by high concentrations of exogenous RNA was also seen when we analyzed GzmB cleavage of hnRNP C1 (Fig. 1E). These results suggest that an excess of nucleic acids interferes with formation of a substrate–nucleic acid–protease complex. Collectively, these results demonstrate that nucleic acid binding is a conserved and functionally important property of leukocyte serine proteases.

DNA binding mediates localization of Gzms to the nucleus

During killer cell attack, the Gzms rapidly concentrate in the nucleus of target cells by an unknown mechanism. A previous study suggested that nuclear localization is mediated by affinity of the Gzms to insoluble NFs (3). We hypothesized that the nuclear accumulation of Gzms is driven by direct binding to nuclear DNA. To test this idea, we incubated fixed and permeabilized HeLa cells with AF488-labeled serine proteases and visualized their localization with fluorescence microscopy (Fig. 5A). As expected, the Gzms stained the cytosol and nucleus, but concentrated in the nucleus. To test whether nuclear accumulation was mediated by DNA binding, we coincubated the Gzms with salmon sperm DNA before adding them to the fixed cells. Incubation with exogenous DNA abolished both cytosolic and nuclear staining of the Gzms (Fig. 5A). We treated fixed cells with DNase and RNase, which modestly reduced nuclear and cytosolic GzmB staining, respectively (Supplemental Fig. 2). DNase treatment did not remove all nuclear DNA, so it may be that GzmB binds to residual nucleic acids after nuclease treatment. Labeled NE also accumulated in the nuclei of fixed cells, in agreement with the known nuclear translocation of this enzyme during NETosis (12). Pancreatic

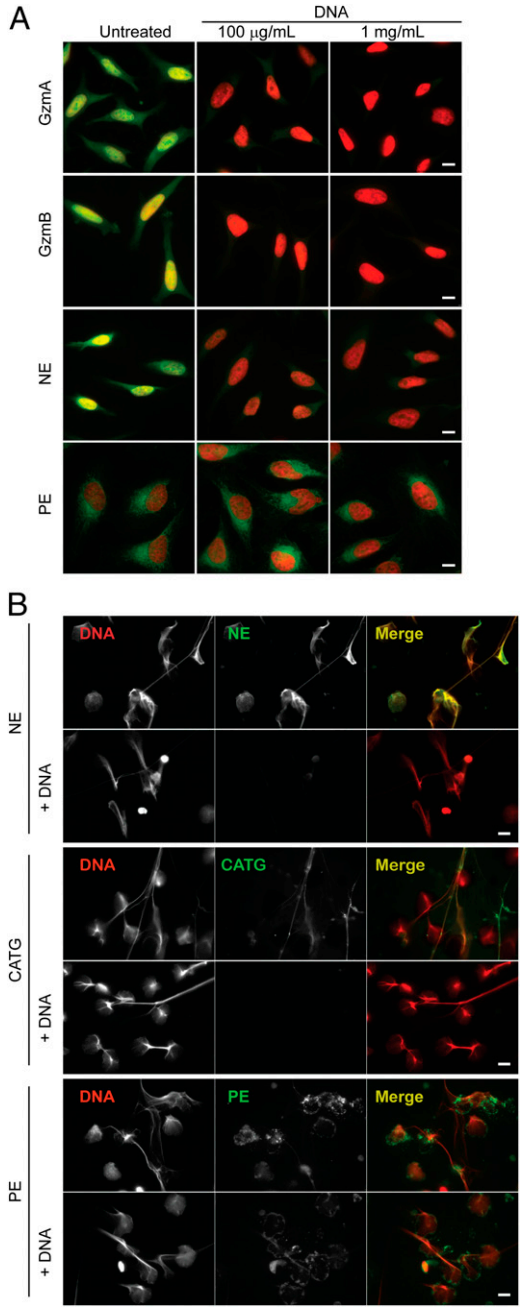

FIGURE 5. DNA binding regulates nuclear localization of leukocyte serine proteases and binding to NETs. The effect of DNA on localization of exogenously added serine proteases to permeabilized cells was assessed by fluorescence microscopy. (**A**) Permeabilized HeLa cells were incubated with AF488-labeled serine proteases (green) that had been preincubated with buffer or DNA and then stained with DAPI (red). GzmA, GzmB, and NE were visualized in the cytoplasm, but concentrated in the nucleus. Preincubation with salmon sperm DNA blocked cellular retention. Pancreatic elastase (PE) did not localize to the nucleus, and its staining pattern was not affected by preincubation with DNA. (**B**) AF488-labeled NE, CATG, and PE (green) were added with or without salmon sperm DNA to neutrophils during NET formation. Cells were fixed and stained for DAPI (red). NE and CATG localized to NETs, but pancreatic elastase did not. Salmon sperm DNA blocked binding of NE and CATG to NETs. Images are representative of three independent experiments. Scale bars, 10 μm.

elastase did not localize to fixed cell nuclei, and its staining intensity and pattern were not impacted by preincubation with salmon sperm DNA (Fig. 5A). Thus, DNA binding by the Gzms and NE likely mediates their nuclear trafficking during cytotoxic attack and NETosis, respectively.

Localization of NE and CATG to NETs is mediated by DNA binding

CATG and NE both concentrate on NETs (13). We asked whether DNA binding facilitates localization of these enzymes to NETs. Neutrophils isolated from human peripheral blood were treated with PMA for 3 h to induce NET formation in the presence of AF488-labeled NE, CATG, or pancreatic elastase. Competitor DNA was added to some samples during NET formation. Both neutrophil enzymes, but not pancreatic elastase, spontaneously concentrated on the NETs, and binding to the NETs was inhibited by adding salmon sperm DNA (Fig. 5B). Exogenous DNA added during NETosis also reduced the association of endogenous NE to NETs (Supplemental Fig. 3). Thus, CATG and NE specifically localize to NETs by binding to DNA.

Discussion

This work demonstrates that the Gzms and related leukocyte proteases are bona fide nucleic acid binding proteins with nanomolar affinities. The basis for substrate specificity of the Gzms, which are highly specific proteases, remains largely unknown. Although each Gzm has a strong preference for specific P1 residues in its substrates, primary amino acid sequence around the cleavage site does not predict Gzm cleavage. Structural features likely play a key role in Gzm substrate recognition. This study suggests that the high affinity of the Gzms for nucleic acids may be an important determinant of substrate specificity. Nucleic acid binding is a simple and elegant mechanism to direct leukocyte serine proteases to DNA and RNA binding protein targets and probably explains why nucleic acid binding proteins are highly overrepresented among Gzm substrates. Gzms and their substrates may be brought together by binding to nearby sites on the same nucleic acid strand. The Gzms form a monophyletic group with other leukocyte serine proteases, which also bind to nucleic acids with high affinity. Importantly, nucleic acid binding regulates the subcellular localization of Gzms and neutrophil proteases. Leukocyte protease concentration in cell nuclei was prevented by exogenous DNA. Our results support the affinity model for Gzm nuclear concentration posited over a decade ago and identify DNA as the unknown insoluble factor mediating this phenomenon (3). Similarly, the localization of NE and CATG to NETs and the antimicrobial activity of NETs likely depend in part upon the affinity of these proteases for DNA.

The leukocyte serine proteases rank among the most cationic proteins in the cell, with very high predicted isoelectric points (pIs): GzmA, 9.22; GzmB, 9.69; CATG, 11.37; and NE, 9.89 (20). The empirical pIs of NE and CATG are ~11 and >11, respectively (30). This raises the question of whether nucleic acid binding is specific or simply a consequence of charge-balancing electrostatic interactions. For several reasons, we believe binding is specific and physiologically relevant. First, the digestive serine proteases, which do not bind nucleic acids, are also cationic with similar pIs as the Gzms. Porcine pancreatic elastase has a reported pI of 9.5 to >11, whereas the pI of trypsinogen is ~9.3, but neither binds nucleic acids (31–33). Secondly, Gzm binding to DNA is sequence specific, favoring pyrimidine oligomers. Third, these proteases directly bind DNA under physiologic conditions. Finally, charge alone does not preclude specificity; RNA and DNA binding proteins are characterized by cationic patches that mediate binding to nucleic acids by electrostatic interactions (34). The Gzm structures predict positively charged surfaces that could be nucleic acid binding sites (35, 36). Further biochemical and structural studies

that look at the interactions of these leukocyte proteases with nucleic acids and specific protein substrates are needed.

Negatively charged sugars play a significant role in granule packaging and target cell uptake of cationic Gzms. In cytotoxic granules, the Gzms bind serglycin, a small negatively charged proteoglycan containing chondroitin 4-sulfate (37). Serglycin-null T cells are defective in packaging GzmB into granules. Upon degranulation, GzmB is released from serglycin and binds to cell membrane proteoglycans, most notably heparan sulfate. Purified GzmB has higher affinity for heparan sulfate than serglycin (38). Our results suggest that when Gzms enter target cells they bind to another class of negatively charged molecules, nucleic acids. Gzm binding to different anionic biomolecules as they move from the granules to the target cell nucleus may form a physical chain of custody to ensure proper Gzm trafficking and targeting.

Nucleic acid binding enhances the activity and function of leukocyte serine proteases, which may be critical to Gzm induction of cell death and neutrophil protease-mediated NET formation and function. Exogenous DNA transformed purified H1 from a very weak substrate to a robust target. However, excess DNA and RNA inhibited cleavage of H1 and hnRNP C1, respectively. A previous study also found that DNA inhibited NE and CATG proteolysis of the nonnucleic acid binding protein elastin (39). An excess of nucleic acid, which has high affinity for both the protease and its substrate, likely interferes with formation of the ternary protease–nucleic acid–substrate complex.

Preferential targeting of DNA and RNA binding proteins by Gzms is an underappreciated property critical for executing cell death. Nucleic acid binding is a simple mechanism to guide Gzms to targets that are essential for survival. Cleavage of nucleic acid binding substrates should enhance Gzm execution of death, independently of caspase activation. During Gzm-mediated cell death, targeting of RBPs disrupts pre-mRNA processing and nuclear export (4). In the extracellular environment, DNA binding may sequester leukocyte serine proteases to focus their activity on pathogens, which get caught in NETs, and minimize tissue injury.

Acknowledgments

We thank Farokh Dotiwala and Nishant Dwivedi for input and technical assistance and Brian Beliveau and Nancy Kedersha for advice and reagents.

Disclosures

The authors have no financial conflicts of interest.

References

1. Chowdhury, D., and J. Lieberman. 2008. Death by a thousand cuts: granzyme pathways of programmed cell death. *Annu. Rev. Immunol.* 26: 389–420.
2. Jans, D. A., P. Jans, L. J. Briggs, V. Sutton, and J. A. Trapani. 1996. Nuclear transport of granzyme B (fragmentin-2). Dependence of perforin in vivo and cytosolic factors in vitro. *J. Biol. Chem.* 271: 30781–30789.
3. Jans, D. A., L. J. Briggs, P. Jans, C. J. Froelich, G. Parasivam, S. Kumar, V. R. Sutton, and J. A. Trapani. 1998. Nuclear targeting of the serine protease granzyme A (fragmentin-1). *J. Cell Sci.* 111: 2645–2654.
4. Rajani, D. K., M. Walch, D. Martinvalet, M. P. Thomas, and J. Lieberman. 2012. Alterations in RNA processing during immune-mediated programmed cell death. *Proc. Natl. Acad. Sci. USA* 109: 8688–8693.
5. Zhang, D., M. S. Pasternack, P. J. Beresford, L. Wagner, A. H. Greenberg, and J. Lieberman. 2001. Induction of rapid histone degradation by the cytotoxic T lymphocyte protease Granzyme A. *J. Biol. Chem.* 276: 3683–3690.
6. Zhu, P., D. Martinvalet, D. Chowdhury, D. Zhang, A. Schlesinger, and J. Lieberman. 2009. The cytotoxic T lymphocyte protease granzyme A cleaves and inactivates poly(adenosine 5′-diphosphate-ribose) polymerase-1. *Blood* 114: 1205–1216.
7. van Domselaar, R., R. Quadir, A. M. van der Made, R. Broekhuizen, and N. Bovenschen. 2012. All human granzymes target hnRNP K that is essential for tumor cell viability. *J. Biol. Chem.* 287: 22854–22864.
8. Knickelbein, J. E., K. M. Khanna, M. B. Yee, C. J. Baty, P. R. Kinchington, and R. L. Hendricks. 2008. Noncytotoxic lytic granule-mediated CD8+ T cell inhibition of HSV-1 reactivation from neuronal latency. *Science* 322: 268–271.
9. Marcet-Palacios, M., B. L. Duggan, I. Shostak, M. Barry, T. Geskes, J. A. Wilkins, A. Yanagiya, N. Sonenberg, and R. C. Bleackley. 2011. Granzyme B inhibits vaccinia virus production through proteolytic cleavage of eukaryotic initiation factor 4 gamma 3. *PLoS Pathog.* 7: e1002447.
10. Krem, M. M., T. Rose, and E. Di Cera. 2000. Sequence determinants of function and evolution in serine proteases. *Trends Cardiovasc. Med.* 10: 171–176.
11. Brinkmann, V., and A. Zychlinsky. 2012. Neutrophil extracellular traps: is immunity the second function of chromatin? *J. Cell Biol.* 198: 773–783.
12. Papayannopoulos, V., K. D. Metzler, A. Hakkim, and A. Zychlinsky. 2010. Neutrophil elastase and myeloperoxidase regulate the formation of neutrophil extracellular traps. *J. Cell Biol.* 191: 677–691.
13. Urban, C. F., D. Ermert, M. Schmid, U. Abu-Abed, C. Goosmann, W. Nacken, V. Brinkmann, P. R. Jungblut, and A. Zychlinsky. 2009. Neutrophil extracellular traps contain calprotectin, a cytosolic protein complex involved in host defense against *Candida albicans*. *PLoS Pathog.* 5: e1000639.
14. Thiery, J., M. Walch, D. K. Jensen, D. Martinvalet, and J. Lieberman. 2010. Isolation of cytotoxic T cell and NK granules and purification of their effector proteins. In *Current Protocols in Cell Biology.* John Wiley & Sons, New York, p. 1-29.
15. Brinkmann, V., B. Laube, U. Abu Abed, C. Goosmann, and A. Zychlinsky. 2010. Neutrophil extracellular traps: how to generate and visualize them. *J. Vis. Exp.* 36: 1724.
16. Van Damme, P., S. Maurer-Stroh, H. Hao, N. Colaert, E. Timmerman, F. Eisenhaber, J. Vandekerckhove, and K. Gevaert. 2010. The substrate specificity profile of human granzyme A. *Biol. Chem.* 391: 983–997.
17. Van Damme, P., S. Maurer-Stroh, K. Plasman, J. Van Durme, N. Colaert, E. Timmerman, P.-J. De Bock, M. Goethals, F. Rousseau, J. Schymkowitz, et al. 2009. Analysis of protein processing by N-terminal proteomics reveals novel species-specific substrate determinants of granzyme B orthologs. *Mol. Cell. Proteomics* 8: 258–272.
18. Berriz, G. F., J. E. Beaver, C. Cenik, M. Tasan, and F. P. Roth. 2009. Next generation software for functional trend analysis. *Bioinformatics* 25: 3043–3044.
19. Carbon, S., A. Ireland, C. J. Mungall, S. Shu, B. Marshall, and S. Lewis; AmiGO Hub; Web Presence Working Group. 2009. AmiGO: online access to ontology and annotation data. *Bioinformatics* 25: 288–289.
20. UniProt Consortium. 2012. Reorganizing the protein space at the Universal Protein Resource (UniProt). *Nucleic Acids Res.* 40(Database issue): D71–D75.
21. Goujon, M., H. McWilliam, W. Li, F. Valentin, S. Squizzato, J. Paern, and R. Lopez. 2010. A new bioinformatics analysis tools framework at EMBL-EBI. *Nucleic Acids Res.* 38(Web Server issue): W695–W699.
22. Zhang, H., S. Gao, M. J. Lercher, S. Hu, and W.-H. Chen. 2012. EvolView, an online tool for visualizing, annotating and managing phylogenetic trees. *Nucleic Acids Res.* 40(Web Server issue): W569–W572.
23. Ryder, S. P., and J. R. Williamson. 2004. Specificity of the STAR/GSG domain protein Qk1: implications for the regulation of myelination. *RNA* 10: 1449–1458.
24. Jantz, D., and J. M. Berg. 2010. Probing the DNA-binding affinity and specificity of designed zinc finger proteins. *Biophys. J.* 98: 852–860.
25. Fialcowitz-White, E. J., B. Y. Brewer, J. D. Ballin, C. D. Willis, E. A. Toth, and G. M. Wilson. 2007. Specific protein domains mediate cooperative assembly of HuR oligomers on AU-rich mRNA-destabilizing sequences. *J. Biol. Chem.* 282: 20948–20959.
26. Park, S., D. G. Myszka, M. Yu, S. J. Littler, and I. A. Laird-Offringa. 2000. HuD RNA recognition motifs play distinct roles in the formation of a stable complex with AU-rich RNA. *Mol. Cell. Biol.* 20: 4765–4772.
27. Nightingale, K. P., D. Pruss, and A. P. Wolffe. 1996. A single high affinity binding site for histone H1 in a nucleosome containing the *Xenopus* borealis 5 S ribosomal RNA gene. *J. Biol. Chem.* 271: 7090–7094.
28. Perera, N. C., O. Schilling, H. Kittel, W. Back, E. Kremmer, and D. E. Jenne. 2012. NSP4, an elastase-related protease in human neutrophils with arginine specificity. *Proc. Natl. Acad. Sci. USA* 109: 6229–6234.
29. Belorgey, D., and J. G. Bieth. 1995. DNA binds neutrophil elastase and mucus proteinase inhibitor and impairs their functional activity. *FEBS Lett.* 361: 265–268.
30. Travis, J., P. J. Giles, L. Porcelli, C. F. Reilly, R. Baugh, and J. Powers. 1979. Human leucocyte elastase and cathepsin G: structural and functional characteristics. *Ciba Found. Symp.* 75: 51–68.
31. Brink, N. G., U. J. Lewis, and D. E. Williams. 1956. Pancreatic elastase: purification, properties, and function. *J. Biol. Chem.* 222: 705–720.
32. Ardelt, W. 1975. Physical parameters and chemical composition of porcine pancreatic elastase II. *Biochim. Biophys. Acta* 393: 267–273.
33. Higaki, J. N., and A. Light. 1985. The identification of neotrypsinogens in samples of bovine trypsinogen. *Anal. Biochem.* 148: 111–120.
34. Shazman, S., and Y. Mandel-Gutfreund. 2008. Classifying RNA-binding proteins based on electrostatic properties. *PLOS Comput. Biol.* 4: e1000146.
35. Estébanez-Perpiña, E., P. Fuentes-Prior, D. Belorgey, M. Braun, R. Kiefersauer, K. Maskos, R. Huber, H. Rubin, and W. Bode. 2000. Crystal structure of the caspase activator human granzyme B, a proteinase highly specific for an Asp-P1 residue. *Biol. Chem.* 381: 1203–1214.
36. Hink-Schauer, C., E. Estébanez-Perpiñá, F. C. Kurschus, W. Bode, and D. E. Jenne. 2003. Crystal structure of the apoptosis-inducing human granzyme A dimer. *Nat. Struct. Biol.* 10: 535–540.
37. Kolset, S. O., and H. Tveit. 2008. Serglycin—structure and biology. *Cell. Mol. Life Sci.* 65: 1073–1085.
38. Raja, S. M., S. S. Metkar, S. Höning, B. Wang, W. A. Russin, N. H. Pipalia, C. Menaa, M. Belting, X. Cao, R. Dressel, and C. J. Froelich. 2005. A novel mechanism for protein delivery: granzyme B undergoes electrostatic exchange from serglycin to target cells. *J. Biol. Chem.* 280: 20752–20761.
39. Duranton, J., D. Belorgey, J. Carrère, L. Donato, T. Moritz, and J. G. Bieth. 2000. Effect of DNase on the activity of neutrophil elastase, cathepsin G and proteinase 3 in the presence of DNA. *FEBS Lett.* 473: 154–156.